nks

Nordisk kernesikkerhedsforskning
Norrænar kjarnöryggisrannsóknir
Pohjoismainen ydinturvallisuustutkimus
Nordisk kjernesikkerhetsforskning
Nordisk kärnsäkerhetsforskning
Nordic nuclear safety research

NKS-161
ISBN 978-87-7893-226-2

Analysis of flow fields, temperatures and ruthenium transport in the test facility

Teemu Kärkelä, Jouni Pyykönen, Ari Auvinen and Joonas Jokiniemi
VTT, Technical Research Centre of Finland

March 2008

Abstract

Ruthenium transport experiments were conducted at VTT during years 2002-2006. Experiments gave information about ruthenium behaviour in air ingress accident conditions. This study complements those experiments with an analysis of the flows and thermal fields in the test system. Temperature profiles were measured at the walls of the experimental facility. Computational fluid dynamics (CFD) simulations used the measured profiles and provided predictions of flows and temperatures inside the furnace. Ruthenium transport was also modelled with CFD.

Thermal characterisation of the reactor demonstrated that buoyancy has a significant role during the cooling after the furnace. A hypothesis of the dominant role of RuO2 and RuO3 condensation on reactor walls gave simulation results that are in accordance with radiotracer measurements of deposition in experiments conducted with furnace at 1500K. Actually, RuO3 does not condensate, but it thermal decomposes to RuO2. This does not seem to have effect on result. Particle formation around the furnace exit could be detected from the comparison of modelling results with the measured profiles. In several other experiments ruthenium behaviour is dominated by other issues. These are related to the complex ruthenium chemistry that includes various surface reactions. Thermal equilibrium indicates significant gaseous RuO4 concentration around 1300 K. It seems that seed particles decreased the catalytic decomposition activity of RuO4 to RuO2 around this temperature pushing the gas concentration towards the equilibrium, and further give rise to gaseous RuO4 transport to low temperatures. At higher temperature increasing mass flow rate of RuO2 particles is likely to catalyse (decomposition) reaction of RuO4 to RuO2.

Key words

ruthenium, nuclear safety, temperature, CFD

NKS-161
ISBN 978-87-7893-226-2

Electronic report, March 2008

The report can be obtained from
NKS Secretariat
NKS-776
P.O. Box 49
DK - 4000 Roskilde, Denmark

Phone +45 4677 4045
Fax +45 4677 4046
www.nks.org
e-mail nks@nks.org

RESEARCH REPORT

NO VTT-R-00947-08 | 1.2.2008

CHEMPC 13180

Analysis of flow fields, temperatures and ruthenium transport in the test facility

Authors: Teemu Kärkelä, Jouni Pyykönen, Ari Auvinen, Joonas Jokiniemi

Confidentiality: Public

Report's title	
Analysis of flow fields, temperatures and ruthenium transport in the test facility	
Customer, contact person, address NKS, Patrick Isaksson, Vattenfall Power Consultant AB P.O. Box 527, SE-162 16 Stockholm, Sweden	Order reference AFT/NKS-R(07)59/6
Project name Primary circuit chemistry of fission products	Project number/Short name 13180 / CHEMPC
Author(s) T. Kärkelä, J. Pyykönen, A. Auvinen	Pages 14 + Appendixes 5
Keywords Ruthenium, temperature, CFD	Report identification code VTT-R-00947-08

Summary

Ruthenium transport experiments were conducted at VTT during years 2002-2006. Experiments gave information about ruthenium behaviour in air ingress accident conditions. This study complements those experiments with an analysis of the flows and thermal fields in the test system. Temperature profiles were measured at the walls of the experimental facility. Computational fluid dynamics (CFD) simulations used the measured profiles and provided predictions of flows and temperatures inside the furnace. Ruthenium transport was also modelled with CFD.

Thermal characterisation of the reactor demonstrated that buoyancy has a significant role during the cooling after the furnace. A hypothesis of the dominant role of RuO_2 and RuO_3 condensation on reactor walls gave simulation results that are in accordance with radiotracer measurements of deposition in experiments conducted with furnace at 1500K. Actually, RuO_3 does not condensate, but it thermal decomposes to RuO_2. This does not seem to have effect on result. Particle formation around the furnace exit could be detected from the comparison of modelling results with the measured profiles. In several other experiments ruthenium behaviour is dominated by other issues. These are related to the complex ruthenium chemistry that includes various surface reactions. Thermal equilibrium indicates significant gaseous RuO_4 concentration around 1300 K. It seems that seed particles decreased the catalytic decomposition activity of RuO_4 to RuO_2 around this temperature pushing the gas concentration towards the equilibrium, and further give rise to gaseous RuO_4 transport to low temperatures. At higher temperature increasing mass flow rate of RuO_2 particles is likely to catalyse (decomposition) reaction of RuO_4 to RuO_2.

Confidentiality	Public

Espoo 1.2.2008

Jukka Lehtomäki
Technology Manager

Ari Auvinen
Senior research Scientist

VTT's contact address
VTT, P.O. Box 1000, FI-02044 VTT, Finland

Distribution (customer and VTT)
VTT Kirjaamo, SAFIR 2010– Tukiryhmä 5, SARNET Source Term WP 14-1, NKS Secretariat

Preface

Transport of ruthenium in air ingress accident has been studied in VTT and several experiments have been conducted during years 2002-2006. As a result a large data base on ruthenium transport has been gathered. In order to be able to conduct modelling on ruthenium transport it is important to have data about temperature profile inside the test facility. Detailed temperature measurements were done during year 2007.

The financial support of the Finnish Research Programme on Nuclear Power Plant Safety (SAFIR), the Fortum Nuclear Services Ltd (FNS) and the Nordic Nuclear Safety Research (NKS) is acknowledged.

Espoo 1.2.2008

Teemu Kärkelä, Jouni Pyykönen, Ari Auvinen, Joonas Jokiniemi

Contents

1 Introduction

Ruthenium transport experiments were conducted during years 2002-2006 in VTT [Backman et al., 2004], [Kärkelä et al., 2007]. Experiments gave a wide range of data about ruthenium behaviour in air ingress accidents conditions. In some experiments gammatracer was used to determine ruthenium deposition profile inside the experimental facility. Measured ruthenium data is used in modelling of ruthenium transport.

However, to be able to conduct modelling on ruthenium transport, it is important to know temperature profile inside the experimental facility. Detailed temperature profile measurements were done during year 2007.

Modelling of ruthenium transport was the last phase in ruthenium study. Modelling was performed to provide an idea of the temperature and flow field in the experimental system. Modelling enabled studying the relative importance of different transport processes on ruthenium behaviour.

2 Experimental facility

2.1 Facility for temperature measurements

The facility used in temperature measurements (in figure 1), was similar as in experiments on ruthenium transport before [Kärkelä et al., 2007], except the sampling lines were not included. Therefore, the facility composed of tubular flow furnace (Entech, ETF20/18IIL), which had 9 holes on the side wall for temperature measurement. Inside the furnace was a high purity alumina tube. It was connected to a stainless steel (SS 316 L) tube at the outlet of the furnace.

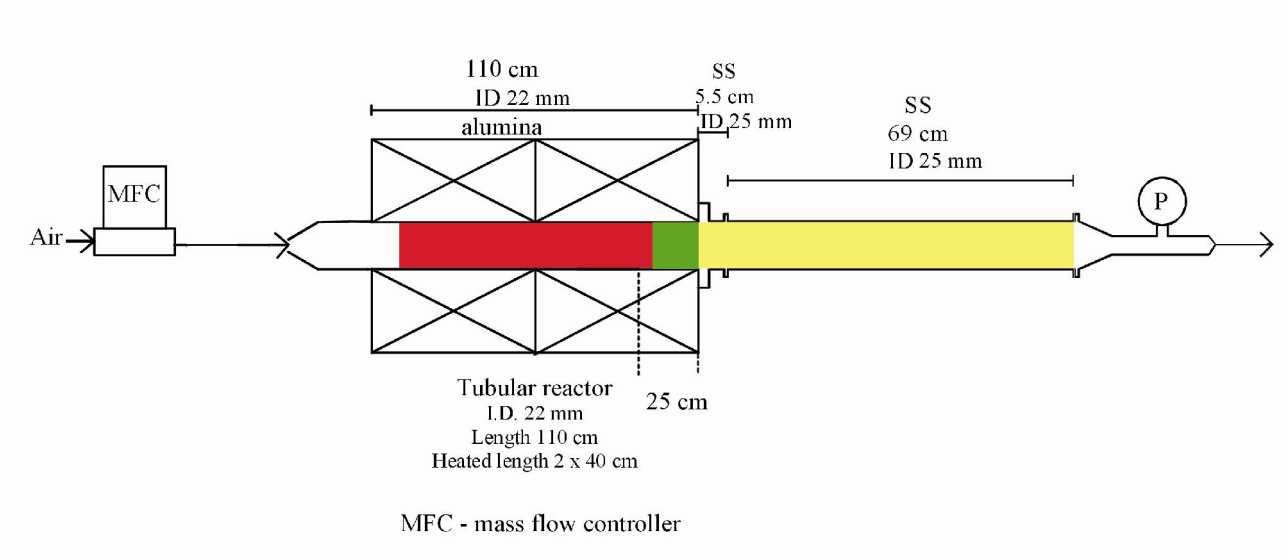

Figure 1. Experimental facility used in temperature measurements.

Air flow through the furnace was controlled with mass flow controller (Brooks 5851S) and flow rate was 5 l/min (NTP, NTP conditions 0°C, 101325 Pa). As air exited the furnace, it cooled in a stainless steel tube. Pressure inside the facility was kept close to atmospheric.

2.2 Locations of thermocouples

Thermocouples used were K-type and B-type. The design A of K-type thermocouples had 1.5 mm tip diameter and design B 3.2 mm. Temperature maximums were 1100°C and 1335°C respectively. B-type thermocouples had 0.7 mm tip diameter and temperature maximum was 1700°C.

Thermocouples were used to measure temperature at three different zones. Those were the surface temperature of alumina tube inside the furnace - red section in figure 1. K-type thermocouples with design B were mounted through 9 holes on the side of the furnace in such a way that their tips were touching the side of the tube.

The second zone was the section of alumina tube, which was inside the insulation at the end of the furnace – green section in figure 1. Six B-type thermocouples were attached on the top surface of alumina tube and two on the bottom surface.

The third zone was stainless steel tube after the furnace – yellow section in figure 1. K-type thermocouples with design A were attached on the inner surface of tube through holes drilled through the tube. Thermocouples were measuring temperature of gas flow on the tube wall. The total number of thermocouples attached on tube was 30, of which four were mounted on stainless steel connector between alumina furnace tube and the stainless steel tube. Temperature was measured on the top, bottom and side surfaces (both left and right) of tube by rotating the tube 180° between experiments.

The locations of thermocouples are presented in table 1. The zero point is at the end of the furnace. Positive direction is downstream from the furnace. So, the insulation at the end of the furnace is located between -14 to 0 cm.

Table 1. The locations of thermocouples used in temperature measurements. The zero point is located at the end of the furnace.

Zone	Thermocouple locations [cm]
Surface temperature of alumina tube side wall inside the furnace	-87, -79, -71, -63, -55, -47, -39, -31, -23, top wall -20, -17
The section of alumina tube inside insulation: Top surface	-14, -10, -5, -1
The section of alumina tube inside insulation: Bottom surface	-14, -5
Stainless steel tube after the furnace: Downstream from the furnace, left side	7.3, 10.3, 13.4, 16.3, 20.3, 24.3, 28.3, 32.3, 39.9, 43.3, 55.3
Stainless steel tube after the furnace: Downstream from the furnace, top side	connector 2.3, 4.2, tube 7.7, 10.4, 13.5, 20.4, 24.8, 28.6, 32.8, 37, 43.6, 55.5, 65.5
Stainless steel tube after the furnace: Downstream from the furnace, right side	connector 2.3, 4.4, tube 7.6, 13.2, 20.5, 28.7

The temperature profile approximately in the middle of gas flow was measured with one thermocouple (design A). It was mounted through special designed connector into stainless steel tube of the experimental facility. The gas temperature measurements were conducted between -9 – 53.5 cm. In the measurements the thermocouple was moved with small increments, approx. 1 cm, from the outlet of stainless steel tube to upstream. The locations of measured points are presented in appendix B.

3 Experiments

Temperature measurements were conducted at 1100, 1300, 1500 and 1700 K furnace set point temperatures, which equal temperatures used in ruthenium transport experiments. Air flow through the furnace was 5 l/min (NTP). The total number of the tests was fifteen. Three of them were repeated tests because of interference in the previous experiment. The experimental matrix is presented in table 2.

Table 2. The experimental matrix of temperature measurements.

Exp. [#]	Furnace set point [K]	Measurement	Other
1	1100	Surface temp.	
2	1300	Surface temp.	
3	1500	Surface temp.	
4	1700	Surface temp.	
5	1100	Surface temp.	180° rotation
6	1300	Surface temp.	180° rotation
7	1500	Surface temp.	180° rotation
8	1700	Surface temp.	180° rotation
9	1100	Gas temp.	
10	1300	Gas temp.	
11	1500	Gas temp.	
12	1700	Gas temp.	
13	1100	Surface temp.	Repeat
14	1300	Surface temp.	Repeat
15	1300	Gas temp.	Repeat

The results of temperature measurements are presented as one minute averages, while the facility was at the operation temperature.

In figure 2 are presented the measured temperature profiles in the experimental facility. The outlet of the furnace is located at 0 cm (compare with figure 1). Temperatures presented in the figure are measured on the top surface, except between -87 - -23 cm, where the side wall was measured. Within the furnace the measurements were conducted on the outer surface and after the furnace on the inner surface of the tube. At 1700 K temperature thermocouples touching the side wall inside the furnace were not used. Average values of the measured temperatures are presented in tables A-1 – A-4 in appendix A.

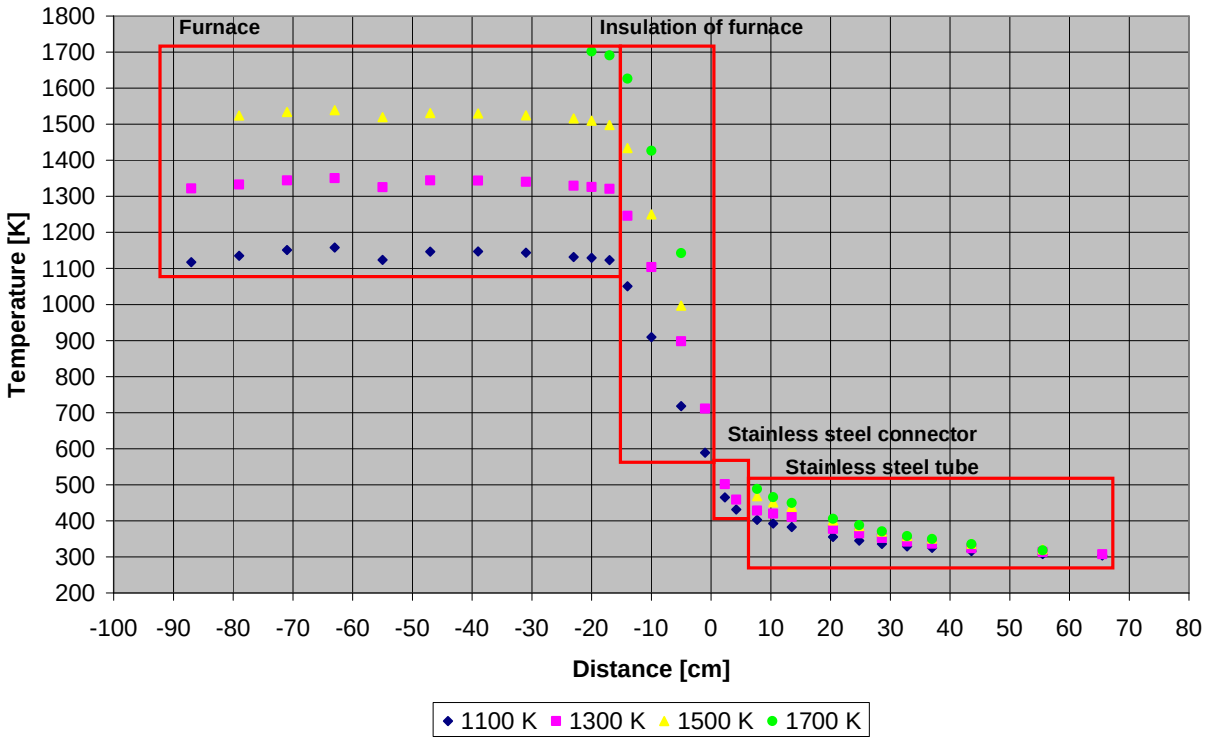

Figure 2. Measured temperature profiles in the experimental facility. Temperatures are measured on the top wall of the tube, except between -87 – -23 cm where the side wall was measured. The outlet of the furnace is located at 0 cm.

It can be seen in figure 2 that temperature is rather constant inside the furnace at location from -45 to -25 cm, where the evaporation crucible was located in ruthenium transport experiments. The insulation of the furnace was located between -14 to 0 cm. Inside the insulation temperature decreased very rapidly. In ruthenium transport experiments temperature gradient caused reactive condensation of gaseous ruthenium species and deposition on the wall of alumina tube as RuO_2. The maximum temperature difference at the end of the insulation between top and bottom surface of alumina tube was 28 K, when the furnace set point was 1700 K.

After the furnace there were stainless steel connector and stainless steel tube. Temperatures inside these parts are presented more accurately in figure 3. Again the outlet of the furnace is located at 0 cm. Gas temperatures are measured at the inner surface on top and bottom wall of tube. The set point of the furnace was 1100 K and 1300 K, when temperature inside the stainless steel connector was measured. Temperature continued to decrease within both sections. Therefore within those sections (range from 0 to 25 cm) in ruthenium transport experiments there was also a lot of ruthenium particle deposition mainly due to thermophoresis. From 25 cm to downstream the temperature decreased further and decomposition of gaseous RuO_4 to solid RuO_2 took place. Decomposition seemed to take place preferably at around 100°C. For comparison temperatures measured at the side walls are presented in figure C-1 of appendix C.

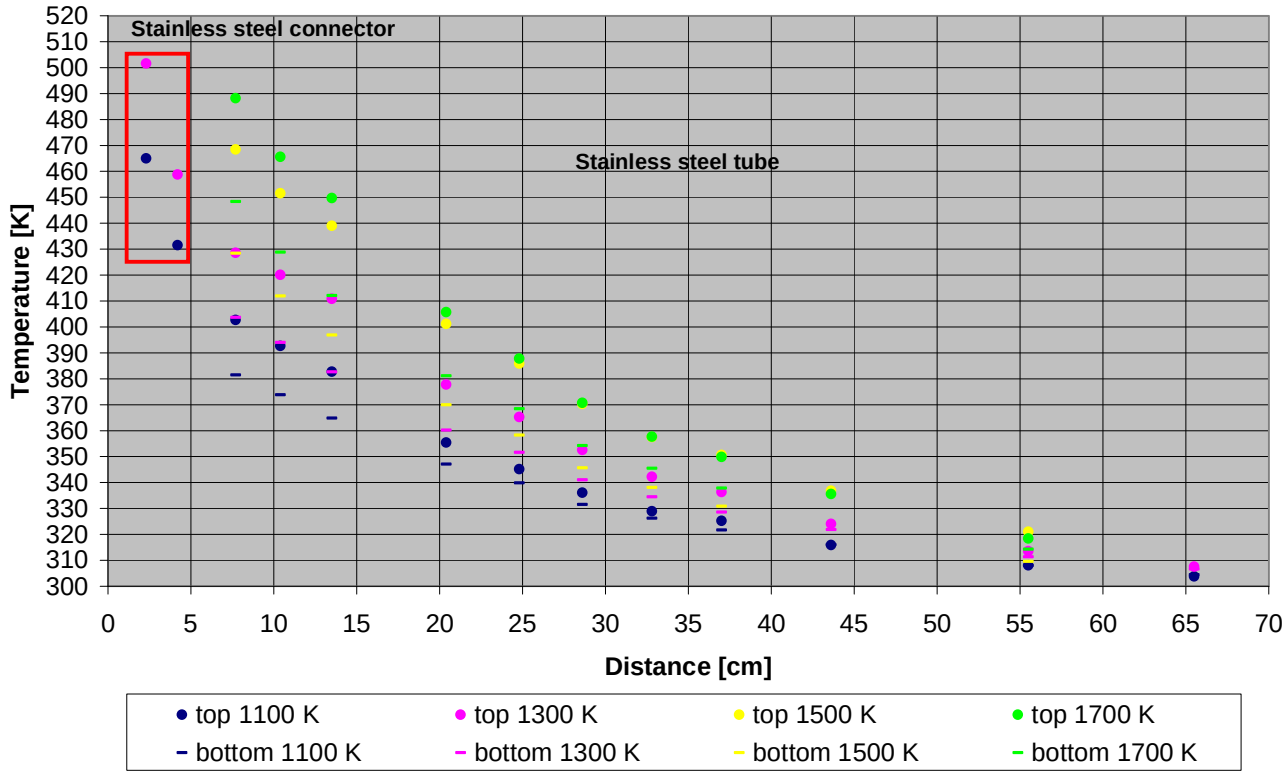

Figure 3. Measured temperatures inside stainless steel connector and tube. Temperatures are measured at the inner surface on top and bottom wall of the tube.

The results of the gas temperature measurements approximately from the middle of the flow channel are presented in appendix B. During the measurements it was noticed that the tip of the thermocouple was not located exactly in the centre of the flow channel all the time. The manufactured supporting frame of the tip did not withstand the heat especially at 1500 K and 1700 K. The tip was located below the middle of the flow channel as the frame bent during the measurements. Due to the uncertainty in the exact location of the thermocouple and the steep temperature gradient the results from gas temperature measurements were not used in modelling. Measured gas temperatures are also presented in figure C-2 of appendix C.

4 Modelling

4.1 Modelling issues

Modelling was done to provide an idea of the temperature and flow fields in the experimental system. Of special interest is the role of buoyancy since the flow rates are rather low and temperature differences rather high. As the experiments were performed in a horizontal reactor, this adds an extra dimension in the interpretation of the results. Modelling studies have been done as computational fluid dynamics (CFD) simulation using a commercial software package Fluent. Another topic considered in the modelling studies was the dissipation of turbulence at the entrance of the furnace. Because of this the computational grid extended right to be beginning of the test facility.

Another objective of modelling was to provide some framework for interpreting the experimental results of ruthenium behaviour in the conditions of interest. As the experiments are directed towards uncharted territory, there is no possibility of a sound mechanistic model of all the phenomena. Establishment of kinetics, even for simple hypothetical reactions, would require more data. Instead, we have modelled a case of purely diffusion-limited case of RuO_2 and RuO_3 transport and deposition to the reactor surfaces. This seemed to be the dominant process in certain cases, and thus, the simulations provide an upper bound for this process.

4.2 Model

The fluid flow simulations cover the whole reactor from the tube entering the reactor until the reactor exit. The computational domain used in the calculations is shown in Fig. 4. The domain was constructed in 3D, and the symmetry enabled us to consider only half of the reactor tube. The domain consists of three parts, the furnace, the insulation, and the outflow. The grid was generated as a structured hexahedral grid. A so called O-grid grid arrangement was adopted. In the region near the inlet and the boundary between the insulation and the outflow parts where high gradients of variables are expected, non-uniform grid distribution was generated. Second-order accurate upwind-discretisation was used to solve the standard fluid flow equations. Standard wall boundary conditions were set with the thermal boundary conditions taken as polynomial fits from the measurements at various temperatures.

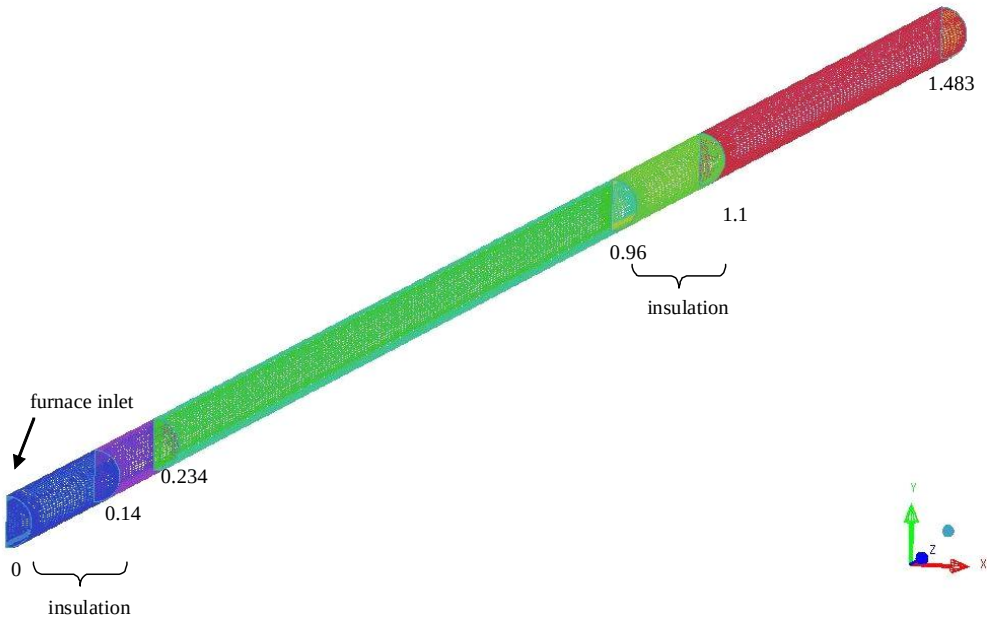

Figure 4. Computational grid of the test facility generated for the modelling studies.

The basic hypothesis in modelling was to study a case of diffusion limited RuO_2 and RuO_3 transport and deposition where the kinetics of ruthenium conversion to RuO_4 is so slow that the conversion is of secondary importance during the relatively brief cooling phase. In reality, the conversion to RuO_4 is not completely insignificant. In any case, we model the behaviour of gaseous RuO_2 and RuO_3 as a separate entity during the cooling phase. In the calculation, we insert all released ruthenium in these two species and consider the role of RuO_4 only in the analysis of the results.

The conversion of ruthenium from the gas phase to the condensed phase is assumed place as reactive condensation of RuO_3 (g) to RuO_2 (c) or as direct condensation of RuO_2. Only condensation on the reactor surfaces was considered by adopting a wall boundary condition of equilibrium concentration above the surface. Neither vapour scavenging by nucleated particles nor possible wall reactions were included in the CFD simulations. An effective total vapour pressure of condensable ruthenium species was calculated with the chemical database system FACT. As we do not allow gaseous RuO_2 and RuO_3 to convert to RuO_4, the effective vapour pressure consists of these two species with the minor species emitted. For simplicity we consider dry air. With steam, RuO_3OH would have a minor, but still appreciable concentration. At any rate, its effect on the effective vapour pressure is not very large (though one can speculate on the role of the OH radical in the kinetics). Since RuO_3 is the dominant species, the effective vapour pressure was calculated by converting the equilibrium concentration of RuO_2 to RuO_3, and adding this to the equilibrium RuO_3 concentration.

The estimation of the diffusion coefficient of the dominant species RuO_3 is somewhat tricky since it does not have a known condensed form. Since the diffusion coefficient estimates of RuO_2 and RuO_4 are close to one another, the estimate of RuO_4 diffusion coefficient, as a lower value of the two, was also adopted for RuO_3.

A number of test cases were run to characterise the flow field. Three cases with furnace temperatures of 1300 K, 1500 K and 1700 K were considered in more detail. Flow rate of 5 L/min was adopted for all of the simulations with ruthenium. The concentration of ruthenium was taken from release rate measurements. The modelled cases correspond closest to experiments 1 (1300 K), A (1500 K) and B (1700 K) in table 2 in the final report of ruthenium transport experiments [Kärkelä et al., 2007]. Therefore the release data of these experiments were adopted.

4.3 Simulation results

CFD simulations that studied the influence of the turbulence entering the reactor showed that, according to the models, inlet turbulence dissipated within the range of concentrations considered. It is still possible that the flow is not perfectly stable even if the model prediction says that practically all turbulence has died out. Most of the experiments were carried out with the flow rate 5 L/min (STP), which is the lowest flow rate. In those conditions, the disturbances are expected to be the smallest.

The predictions of the thermal field are presented in Figs 5 and 6 as vertical cross-cuts from the middle of the tube. In all figures, the vertical dimension has been scaled ten times in relation to the horizontal (i.e. axial) one. The overall features of the results are very close to each other at furnace temperatures 1300 K (Fig. 6) and 1700 K (Fig. 6). It can be noted that buoyancy, indeed, plays a role. The hot gas flow is directed towards the top of the furnace. This means that the top surface of the reactor is more prone to deposition and reaction with the hot gas flow.

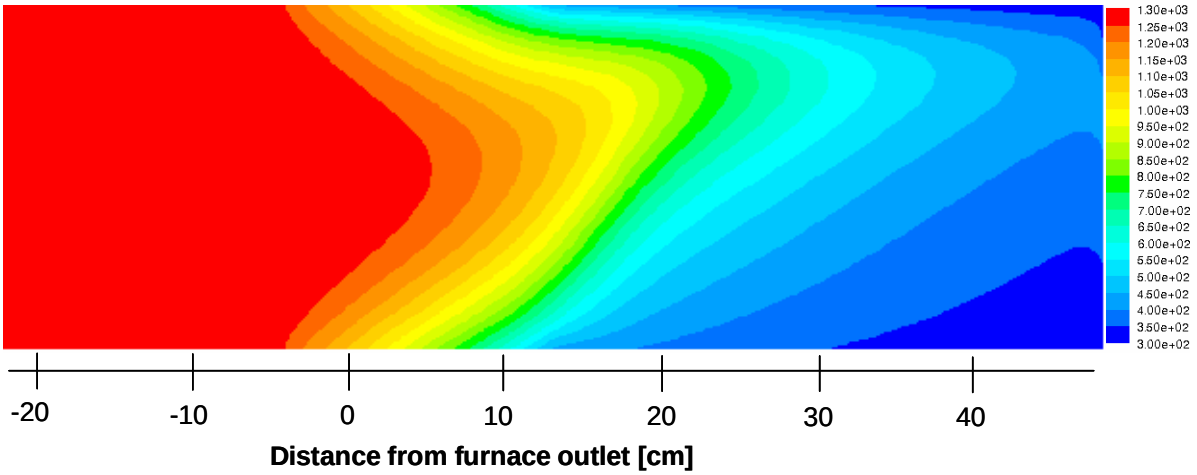

Figure 5. Temperature contours in the case of furnace temperature at 1300 K.

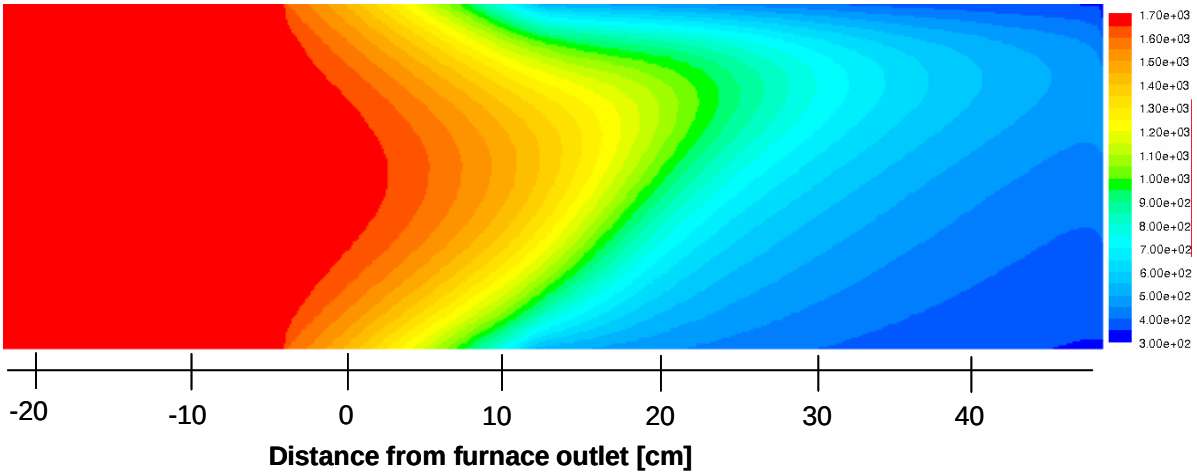

Figure 6. Temperature contours in the case of furnace temperature at 1700 K.

Model predictions of gas ruthenium concentrations (as RuO_3) are shown in Figs 7 - 9. Once again, the features of the contours are rather similar irrespective of the maximum temperature in the furnace, and buoyancy can be observed in the figures. The sharp beginning of wall deposition is clearly visible. Looking at these contours and those of temperature, it seems that part of nucleation takes place rather close to the upper wall of the tube. These particles have a rather high propensity of ending up as wall deposits. In general, the low Reynolds number of the flow can be seen in the relatively short distance where much of the ruthenium vapour depletion takes place.

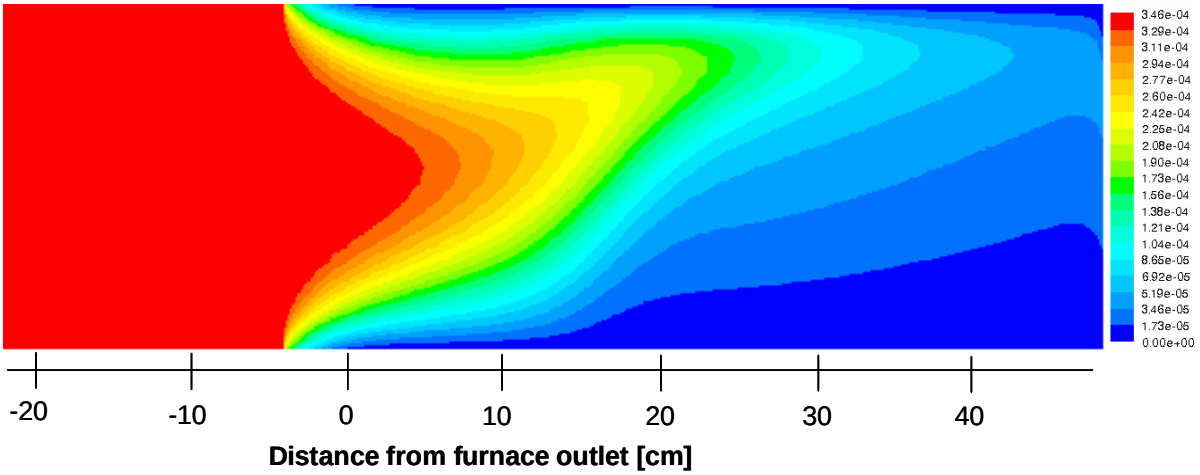

Figure 7. RuO_3 mass fraction in the case of furnace temperature at 1300 K.

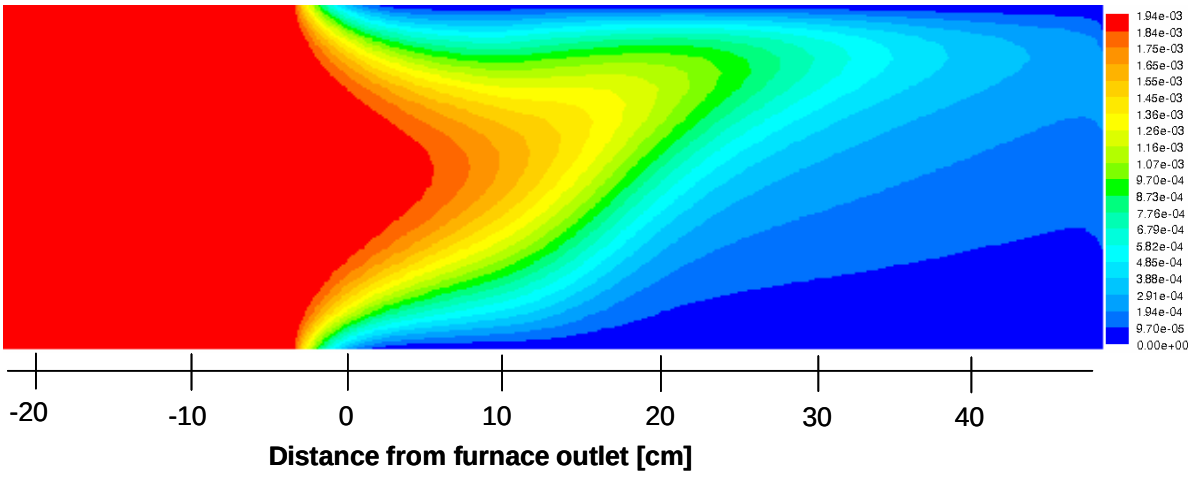

Figure 8. RuO_3 mass fraction in the case of furnace temperature at 1500 K.

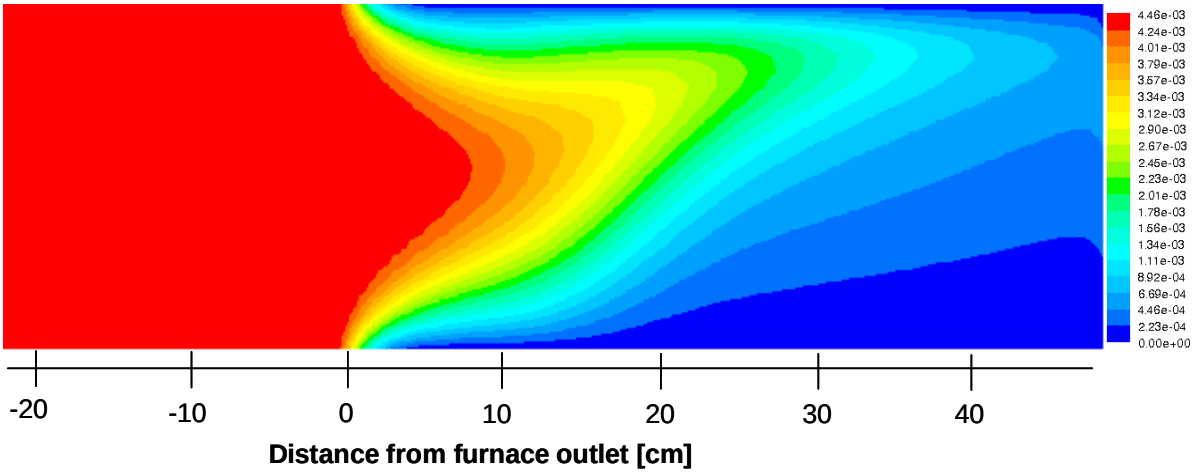

Figure 9. RuO_3 mass fraction in the case of furnace temperature at 1700 K.

The results of the diffusion-limited RuO_3 simulation can be compared against the radiotracer measurements of deposition profiles. The simulated deposition profiles and experimental data are presented Fig. 10. The computational grid is rather coarse and here the retrieval of this data introduces some additional numerical error. Therefore no conclusions should be made based on the exact shapes of the

peaks or the occurrence of minor peaks. The comparison shows that there is reasonable agreement with the experimental data in case of experiments conducted with the furnace at 1500 K. It seems that in these conditions the hypothesis of the dominant roles of RuO_2 and RuO_3 is valid. Particle formation can be observed in the comparison of the simulations and the experimental data. Particles start to have an impact at the furnace outlet (0 cm). Based on pure vapour diffusion, deposition rates should level off at this location. It seems logical that, in reality, most of the RuO_2 and RuO_3 vapour is scavenged by particles here, and that is why the deposition rates decrease further. There is a visible peak of particle deposition due to thermophoresis in the experimental data. Based on the simulations, this mainly originates from the top of the furnace. The fact that experimentally observed level of deposition is much lower at 1300 K than at 1500 K is most likely at least partly due to greater gas phase RuO_4 concentration at that temperature. In equilibrium, RuO_4 mass fraction of gas phase ruthenium species is 25 % at 1300 K, while only 9 % at 1500 K. Even if the experiments show that equilibrium is not reached in the RuO_4 to RuO_3 reaction, it does not necessarily mean that the reaction from RuO_3 to RuO_4 could not approach the equilibrium within the time scale of the heated furnace. However, this scenario is far from a complete explanation for the observed RuO_4 transport rates.

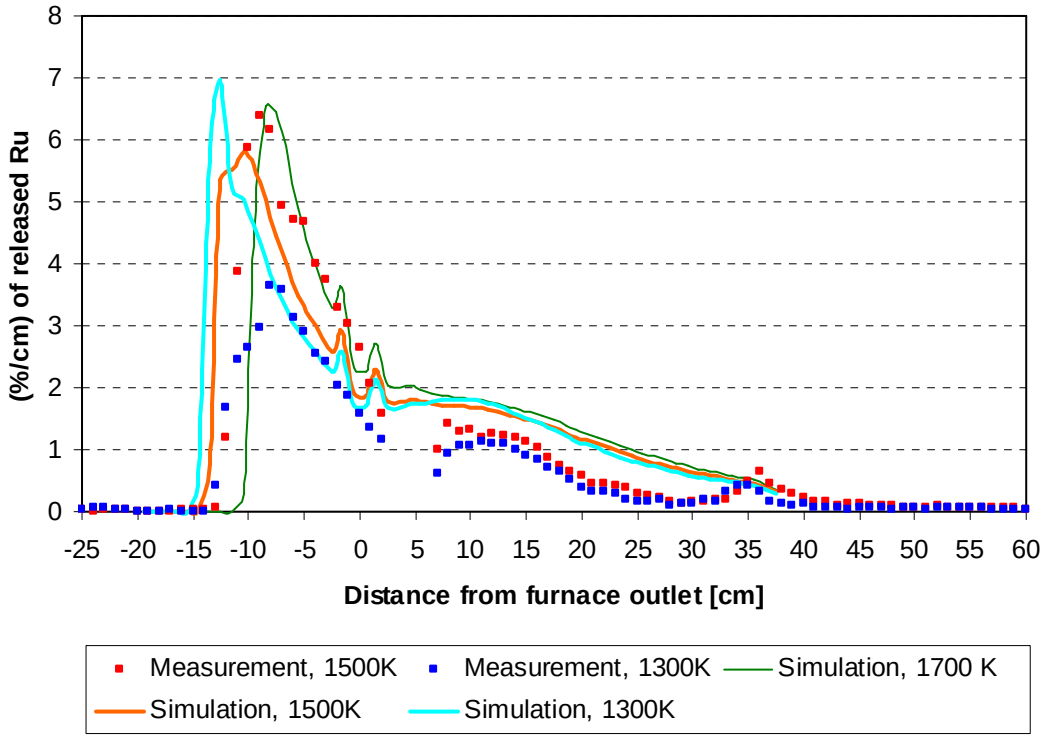

Fig 10. Simulated deposition profiles and comparison with measurements.

5 Conclusions

Experimental studies conducted during 2002-2006 provided an extensive database on ruthenium behaviour in various conditions expected in an air ingress accident.

The chemistry of ruthenium oxides proved to be complex with a number of reaction pathways in gas phase and on the surfaces. Particle formation, impurities and gas composition all played an important role in the experiments.

According to the modelling study diffusion-limited reactive condensation of RuO_3 and direct condensation of RuO_2 seemed to explain majority of the wall deposition observed in the experiments. Particle formation and subsequent thermophoretic deposition especially at the part of the tube close to the outlet of the furnace are likely to explain majority of the remaining differences between the calculated and measured results.

The conclusions that this study allows to make is that wall condensation and particle formation are the dominant processes, when the cooling rate is relatively fast. As the cooling rate was fast in every experiment, it is harder to extend the understanding beyond the conditions encountered in the test facility.

According to thermal equilibrium, there should be significant gaseous RuO_4 concentration especially at the temperature of 1300 K. This would explain the overestimated wall deposition at that temperature. At higher temperature increasing mass flow rate of RuO_2 particles is likely to catalyse decomposition reaction of RuO_4 to RuO_2. Impurities in the gas flow seemed to decrease the catalytic activity and increase the transport of gaseous RuO_4 through the facility.

References

Backman U., Lipponen M., Auvinen A., Jokiniemi J. and Zilliacus R. Ruthenium behaviour in severe nuclear accident conditions – Final Report. VTT Processes, PRO3/P26/04, 2004.

Kärkelä T., Backman, U., Auvinen, A., Zilliacus, R., Lipponen, M., Kekki, T., Tapper U., Jokiniemi, J. Experiments on the behaviour of ruthenium in air ingress accidents – Final Report. VTT TK504, VTT-R-01252-07, 2007.

Appendix A. Average values of measured wall temperatures in the facility

Table A-1. Average outer surface temperatures measured within the furnace at the side wall (sw) and on the top wall (top).

		Furnace set point			
		1100 K	**1300 K**	**1500 K**	**1700 K**
Distance from the outlet [cm]	Location sw/top	Measured temperature [K]			
-87	sw	1117.22	1321.68	-	-
-79	sw	1135.29	1332.81	1523.99	-
-71	sw	1151.15	1343.92	1533.56	-
-63	sw	1157.78	1350.32	1539.22	-
-55	sw	1123.65	1325.48	1519.31	-
-47	sw	1146.58	1344.00	1531.15	-
-39	sw	1147.34	1343.69	1529.95	-
-31	sw	1143.91	1339.97	1524.72	-
-23	sw	1131.72	1329.36	1516.13	-
-20	top	1129.51	1326.07	1509.87	1701.48
-17	top	1122.88	1320.87	1497.88	1690.77
-14	top	1050.73	1245.84	1434.06	1626.39
-10	top	909.72	1103.83	1249.75	1426.54
-5	top	718.23	897.84	997.00	1142.55
-1	top	589.29	711.28	-	-

Table A-2. Average inner surface temperatures measured after the furnace on top wall of the stainless steel connector and tube.

		Furnace set point			
		1100 K	**1300 K**	**1500 K**	**1700 K**
top wall	Distance from the outlet [cm]	Measured temperature [K]			
	2.3	465.03	501.60	-	-
	4.2	431.49	458.75	-	-
	7.7	402.66	428.58	468.49	488.25
	10.4	392.68	420.09	451.53	465.60
	13.5	382.77	410.84	438.97	449.66
	20.4	355.45	377.81	401.19	405.72
	24.8	345.19	365.29	385.88	387.82
	28.6	336.04	352.53	370.29	370.73
	32.8	328.89	342.21	357.49	357.69
	37	325.19	336.34	350.61	349.84
	43.6	315.88	324.05	336.81	335.56
	55.5	308.05	313.57	321.02	318.42
	65.5	303.79	307.55	-	-

Table A-3. Average inner surface temperatures measured after the furnace on bottom wall of the stainless steel connector and tube.

		Furnace set point			
		1100 K	**1300 K**	**1500 K**	**1700 K**
bottom wall	Distance from the outlet [cm]	Measured temperature [K]			
	7.7	381.52	403.66	428.43	448.37
	10.4	373.85	393.99	411.90	428.80
	13.5	364.88	382.67	396.89	412.10
	20.4	347.11	360.20	369.96	381.17
	24.8	339.84	351.63	358.25	368.47
	28.6	331.51	341.03	345.69	354.22
	32.8	326.22	334.47	338.10	345.52
	37	321.71	328.62	330.86	337.88
	43.6	316.08	321.86	-	-
	55.5	307.95	311.34	309.60	314.32
	65.5	304.45	306.65	-	-

Table A-4. Average inner surface temperatures measured after the furnace on side walls of stainless steel tube.

	Left side				Right side			
	Furnace set point				Furnace set point			
	1100 K	1300 K	1500 K	1700 K	1100 K	1300 K	1500 K	1700 K
Distance from the outlet [cm]	Measured temperatures [K]							
2.3	-	-	-	-	449.88	490.29	-	-
4.4	-	-	-	-	421.05	452.16	-	-
7.3	390.39	414.25	454.83	474.14	-	-	-	-
7.6	-	-	-	-	388.05	413.93	449.11	467.88
10.3	380.86	405.72	438.49	452.28	-	-	-	-
13.2	-	-	-	-	372.50	398.36	422.45	433.24
13.4	369.37	394.26	420.79	430.86	-	-	-	-
16.3	359.73	383.34	408.07	414.57	-	-	-	-
20.3	348.42	369.46	-	395.65	-	-	-	-
20.5	-	-	-	-	353.59	376.15	394.85	401.01
24.3	338.16	355.21	373.06	375.56	-	-	-	-
28.3	329.96	344.19	361.01	361.92	-	-	-	-
28.7	-	-	-	-	331.15	346.61	359.13	360.30
32.3	324.71	336.67	350.54	351.06				
36.9	320.96	332.02	345.38	345.25				
43.3	315.62	324.30	334.69	333.79				
55.3	306.14	311.35	317.66	316.29				

Appendix B. Average values of measured gas temperatures in the facility

Table B-1. The measured gas temperatures approximately at the centre of the flow channel.

	Furnace set point			
	1100 K	**1300 K**	**1500 K**	**1700 K**
Distance from the outlet [cm]	Measured gas temperature [K]			
-9	995.12	1150.82	-	-
-8	976.55	1123.78	1238.28	-
-6	939.83	1072.36	1159.66	-
-4	902.01	1019.88	1089.16	1225.05
-3	-	-	-	1178.97
-2	864.11	964.51	1010.01	1127.30
-1	-	-	-	1075.77
0	826.50	915.74	919.05	1020.53
1	812.26	-	876.31	972.25
2	796.51	881.37	840.03	932.59
3	779.86	-	798.09	893.90
4	756.15	843.47	762.51	852.71
5	-	-	722.19	818.47
6	700.88	794.29	673.88	778.56
7	-	-	645.86	739.35
8	632.75	716.55	609.55	700.23
9	-	-	588.28	661.88
10	-	-	576.74	638.83
12	573.80	636.85	556.79	611.86
14	-	-	-	588.47
16	538.52	589.21	-	-
18	-	-	511.53	547.02
20	509.71	551.06	-	-
22	-	-	475.38	507.82
24	476.05	511.78	-	-
26	-	-	449.90	481.72
28	448.56	480.71	-	-
30	-	-	431.23	459.10
32	424.72	454.06	-	-
34	-	-	416.49	441.05
36	402.45	426.47	-	-
38	-	-	402.09	422.28
40	386.49	406.15	-	-
42	-	-	390.20	407.45
46	-	-	379.16	396.35
50	-	-	369.98	385.14
53.5	-	-	363.59	376.36

Appendix C. Figures of measured temperatures

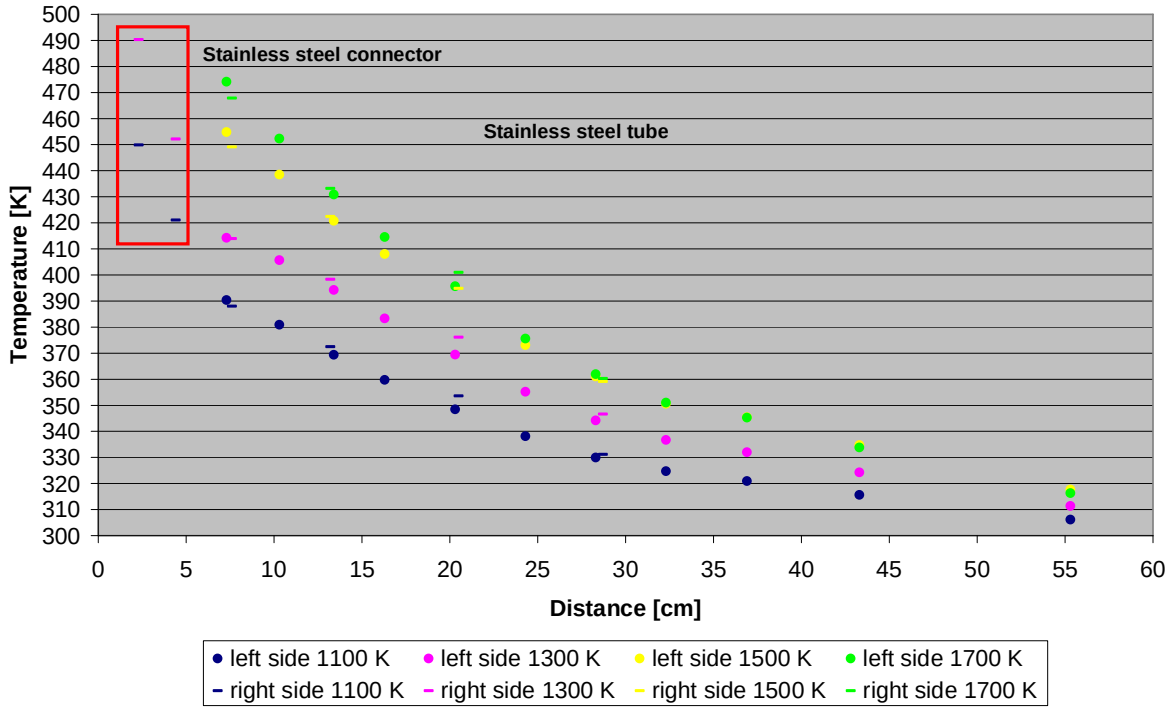

Figure C-1. Measured temperatures inside stainless steel connector and tube. Temperatures are measured at the inner surface on the side walls of the tube.

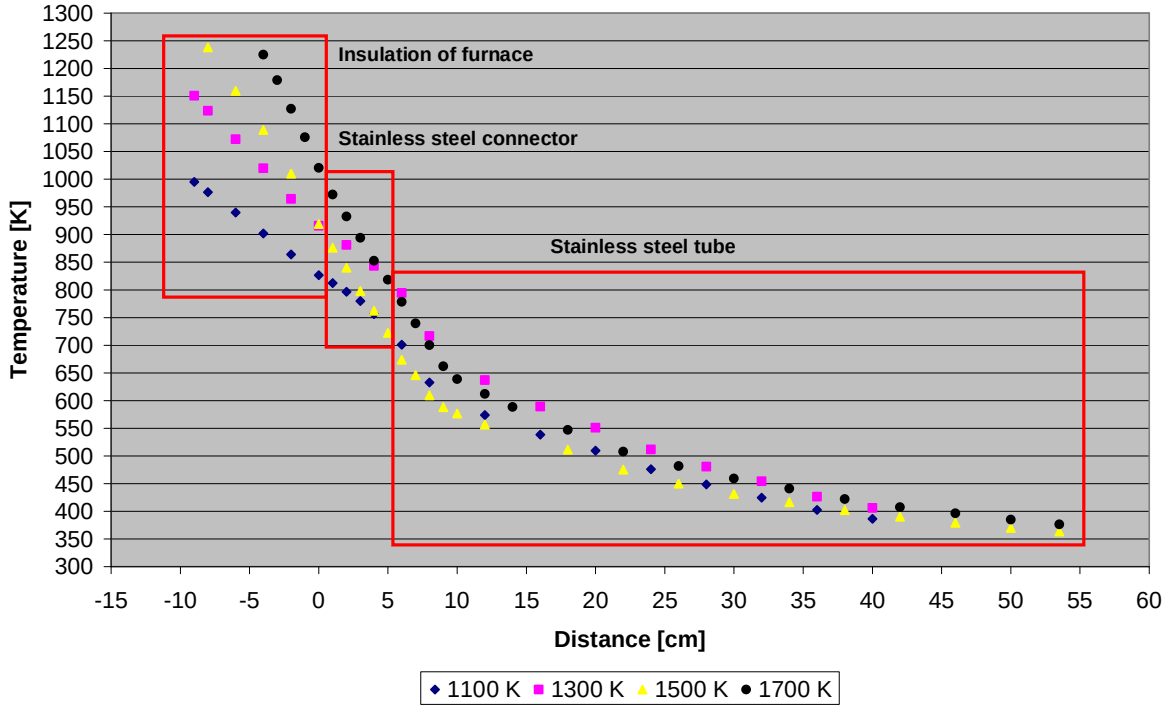

Figure C-2. Measured gas temperatures approximately at the centre of the flow channel with furnace set point ranging from 1100 K to 1700 K.

Title	Analysis of flow fields, temperatures and ruthenium transport in the test facility
Author(s)	Teemu Kärkelä, Jouni Pyykönen, Ari Auvinen and Joonas Jokiniemi
Affiliation(s)	Technical Research Centre of Finland VTT, Fine Particles
ISBN	978-87-7893-226-2
Date	March 2008
Project	NKS-R / Ruthenium Release
No. of pages	14+5
No. of tables	7
No. of illustrations	12
No. of references	2

Abstract

Ruthenium transport experiments were conducted at VTT during years 2002-2006. Experiments gave information about ruthenium behaviour in air ingress accident conditions. This study complements those experiments with an analysis of the flows and thermal fields in the test system. Temperature profiles were measured at the walls of the experimental facility. Computational fluid dynamics (CFD) simulations used the measured profiles and provided predictions of flows and temperatures inside the furnace. Ruthenium transport was also modelled with CFD

Thermal characterisation of the reactor demonstrated that buoyancy has a significant role during the cooling after the furnace. A hypothesis of the dominant role of RuO2 and RuO3 condensation on reactor walls gave simulation results that are in accordance with radiotracer measurements of deposition in experiments conducted with furnace at 1500K. Actually, RuO3 does not condensate, but it thermal decomposes to RuO2. This does not seem to have effect on result. Particle formation around the furnace exit could be detected from the comparison of modelling results with the measured profiles. In several other experiments ruthenium behaviour is dominated by other issues. These are related to the complex ruthenium chemistry that includes various surface reactions. Thermal equilibrium indicates significant gaseous RuO4 concentration around 1300 K. It seems that seed particles decreased the catalytic decomposition activity of RuO4 to RuO2 around this temperature pushing the gas concentration towards the equilibrium, and further give rise to gaseous RuO4 transport to low temperatures. At higher temperature increasing mass flow rate of RuO2 particles is likely to catalyse (decomposition) reaction of RuO4 to RuO2

Key words ruthenium, nuclear safety, temperature, CFD

Available on request from the NKS Secretariat, P.O.Box 49, DK-4000 Roskilde, Denmark.
Phone (+45) 4677 4045, fax (+45) 4677 4046, e-mail nks@nks.org, www.nks.org